Development of Transient Differential Model of Bell-Delaware Method with A Case Study of Water/TiO_2 Nanofluid

A.S. Pereira, M.L. Magalhães and S.J.M. Cartaxo*

Department of Chemical Engineering, Federal University of Ceará, Brazil

Abstract: Heat exchangers are equipments designed for efficient and economic thermal energy transfer between chemical process flows, being widely applied in chemical plants, petrochemical, refinery and power plants. This work aims the development of a rigorous transient model for a 1-2 shell-and-tube of heat exchangers with fractionated baffles, implementing Bell-Delaware method to determine the thermal and fluid dynamics parameters like heat transfer coefficients and pressure drop. For this, Bell-Delaware method has been utilized to the shell-side, considering several types of baffle leaks and its configuration, bypass effect in tube bundles, different input and output distances of baffles, laminar flow, temperature gradient and viscosity variation near the tubes walls. Nanofluid physical properties were locally evaluated by adapted prediction equations available in databases and literature. The case study simulations were performed using the Python computer program and its modules, to determine temperature and physical properties and profiles of TiO_2 nanofluid through the tube, considering a one-dimensional variation, and showing the model applicability for dimensioning and analysis of shell-and-tube 1-2 exchangers.

Keywords: Bell-Delaware, nanofluid, Python, rigorous model.

1. INTRODUCTION

Multitubular heat exchangers, known as shell-and-tubes, emerged at the beginning of the century to fulfill the needs of the oil industry and power plants, as Taborek [1] states.

Colburn [2] was responsible for the first heat transfer coefficient correlation in ideal tube bundles for turbulent flow, which was modified later to include the non-isothermal effects, proposed by Sieder and Tate [3]. Even so, the transfer coefficient for shell-side has proved inefficient in real projects, so Tinker [4] suggested the concept of flow subdivision, which considers the cross-flow, bundle-shell bypass and baffle-shell and baffle-tube leaks.

Bell's method [5] is based on the streams model set by Tinker; however independent factors have been utilized for correcting the heat transfer basic equation and pressure drop on the ideal tube bundle, extended to the intermediary and laminar flow regions. This method provides more accurate results when compared to Kern and Tinker methods and that is why it is considered the most recommended for practical engineering applications, according to Ribeiro [6] and Taborek [1].

2. METHODOLOGY

In this work, central concepts and the calculation routine for estimation of the heat exchange coefficient and pressure drop are presented according to the Bell-Delaware method. To improve the accuracy of the developed differential model, will be used temperature, dependent equations for prediction of physical properties and nanofluids friction factor.

The equations of the mathematical model were numerically solved using a program implemented in Python / IPython Notebook language, associated with some of their scientific modules (math, scipy, numpy and matplotlib).

2.1. Bell-Delaware Method

The method proposed by Tinker [7] to determine the shell-side film coefficient was improved by Bell [5], resulting in a semi-analytical method. Tinker suggested splitting the flow into five individual streams, as illustrated in Figure **1**.

These streams interact with each other, requiring complex modeling, which renders accurate real flow calculations impracticable. Nevertheless, Bell-Delaware method is based on empirical thermo-fluid dynamics performance data, where fluid flow and the heat transfer over ideal tube bundles were studied. Starting from an ideal behavior, some mechanical changes found in commercial heat exchangers were introduced, and the impact on the thermal performance was evaluated.

According to Bell-Delaware method, the pressure drop on the shell-side is due to cross flow contribution, delimited by the edges of two adjacent baffles, but also

*Address correspondence to this author at the Federal University of Ceará, Department of Chemical Engineering; Tel: +558533669611;
Fax: +558533669610; E-mail: samuel@ufc.br

E-ISSN: 2409-5826/15

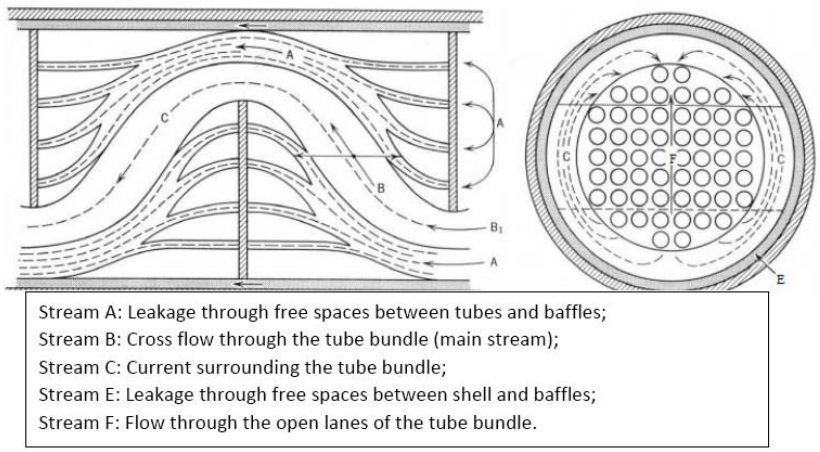

Figure 1: Shell-side streams. Source: Taborek (1983).

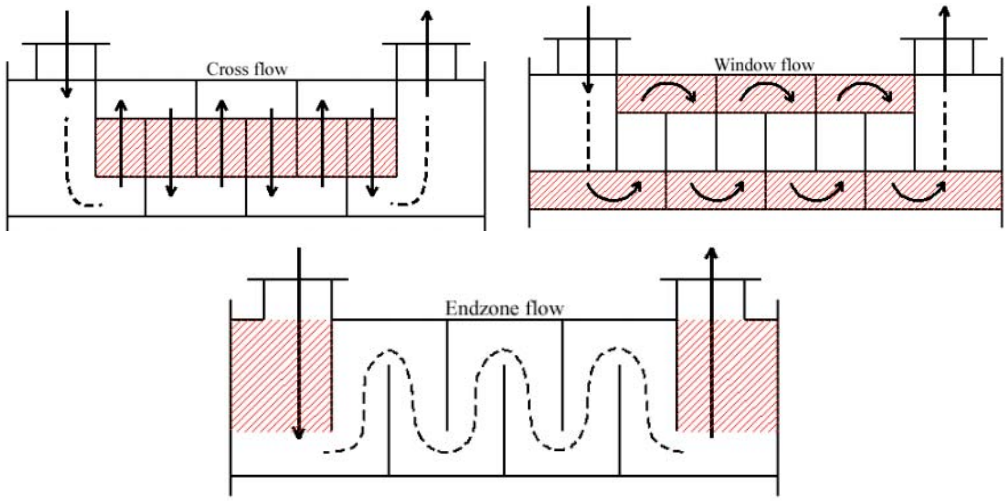

Figure 2: Shell-side pressure drop. Source: Wolverine Company (1984).

due to the window flow between baffles and the input and output areas of the shell-side, as shown in Figure **2**.

In Bell's work [8], the correcting factors for ideal flow heat transfer correlations and the shell-side pressure drop model are both defined. Taborek [1] provides details of the Bell-Delaware method, which presents Equation (1) as the actual shell-side heat transfer coefficient and Equation (2) as pressure drop.

$$hc = \left(J_c.J_L.J_b.J_R.J_S.J_\mu\right).h_{ideal} \quad (1)$$

$$\Delta P_{total} = \Delta P_C + \Delta P_W + \Delta P_e \quad (2)$$

The described method is used to calculate the film coefficient and shell-side pressure drop, while the correlations recommended by the Kern's method can be applied satisfactorily for tubes.

2.2. Physical Properties for Nanofluids

The nanofluid physical properties were assessed at different concentrations and temperatures using empirical correlations. A general weighted mixing rule was used to estimate the density of a nanofluid, as in Equation (3). A specific heat correlation was proposed by Xuan and Roetzel's [9] (Equation (4)).

$$\rho_{nf} = (1-\phi).\rho_f + \phi.\rho_p \quad (3)$$

$$Cp_{nf} = \frac{\phi.\rho_p.Cp_p + (1-\phi).\rho_f.Cp_f}{\rho_{nf}} \quad (4)$$

Equations (5) and (6) provide estimations of viscosity and thermal conductivity, respectively, developed for water-based nanofluids by Sharma *et al*. [10], using empirical data from various researchers. These equations can be used to estimate properties of metal oxides dispersed in water with a concentration of

$\phi \leq 4\%$, liquid temperature $T \leq 70\ ^{\circ}C$ and particle diameter , $d_p \leq 170\ nm$.

$$\mu_{nf} = \mu_f . \left(1 + \frac{\phi}{100}\right)^{11,3} . \left(1 + \frac{T_{nf}}{70}\right)^{-0,038} . \left(1 + \frac{d_p}{170}\right)^{-0,061} \quad (5)$$

$$k_{nf} = 0.8938\, k_f . \left(1 + \frac{\phi}{100}\right)^{1.37} . \left(1 + \frac{T_{nf}}{70}\right)^{-0,2777} . \left(1 + \frac{d_p}{170}\right)^{-0.0336} . \left(\frac{\alpha_p}{\alpha_f}\right)^{-0.0336} \quad (6)$$

2.3. Friction Factor for Nanofluids

Azmi *et al*. [12] proposed Equation (7) to evaluate the friction factor for a TiO_2/water nanofluid over twisted tape inserts, valid in the following conditions: $6800 < Re < 30000$, $5.00 \leq Pr \leq 7.24$, $\phi \leq 3\%$ e $5 \leq (H/D) \leq 15$.

$$\frac{f_{nf}}{f} = 1.4 \left(0.001 + \frac{\phi}{100}\right)^{0.05} \quad (7)$$

The pipe friction factor was directly evaluated using modified physical properties accounting for the deviations caused by the presence of the nanoparticles. For the shell fluid, the following equations were obtained by data regression, where Equation (8) and (9) yielded standard deviations of 0.00002 and 0.0033, respectively.

$$f_{shell} = \left(\left(1.56487.\mathrm{Re}_{shell}^{-0.175}\right)^{1/0.237} + \left(51.36493.\mathrm{Re}_{shell}^{-0.943}\right)^{1/0.237}\right)^{0.237} \quad (8)$$

$$f_{tube} = \left(\left(63.85951.\mathrm{Re}_{tube}^{-0.976}\right)^{1/0.066} + \left(0.45017.\mathrm{Re}_{tube}^{-0.267}\right)^{1/0.066}\right)^{0.066} \quad (9)$$

The friction factor for each 180° fluid return is also an exponential function evaluated in the form:

$$f_{return} = 0.00124.G_{tube}^{1.88683} \quad (10)$$

3. MATHEMATICAL MODEL

The mathematical model is comprised of a set of differential equations obtained from energy balances for each fluid pass through the heat exchanger. Fluid physical properties, friction factor and overall heat transfer coefficients are evaluated locally and all variables and parameters are defined in SI units. The assumptions under which the model is developed are listed below:

- Heat exchanger type is a shell and tube with one shell pass and two tube passes.
- Energy balances assume the allocation of the hot fluid in the shell-side and cold fluid in the tube-side.
- Fluids are in the liquid state, with no phase transition.
- One-dimensional temperature variation.
- Counter-flow inlets.
- Wall conductive resistance negligible.
- The shell is thermally isolated from the environment.
- Newtonian fluids.

The equation development followed the balance over an infinitesimal control volume transversal to the heat exchanger axis, and with thickness *dx*, as shown in Figure **3**. Implementing the energy balances using a truncated Taylor series expansion along the *x* coordinate and disregarding heat capacity changes for infinitesimal space and time variations, we obtain the following differential equations:

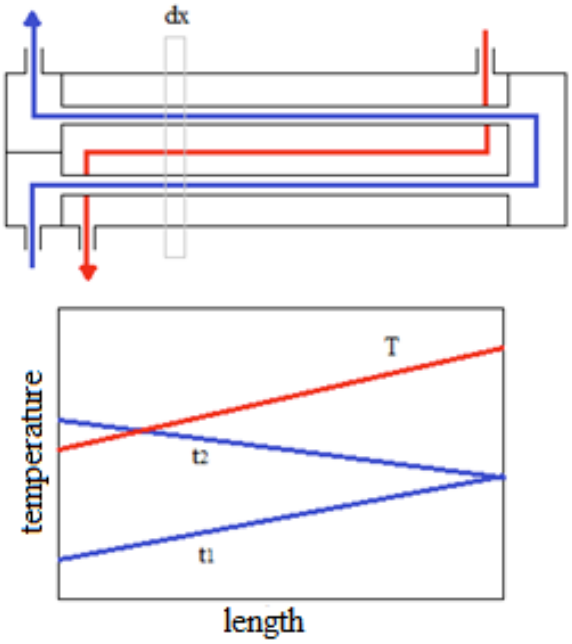

Figure 3: Representation of a 1−2 shell-and-tube heat exchanger.

- **Energy balance for the first tube-side pass**

$$\frac{\partial(t_1)}{\partial t} = \frac{-w.cp_t \frac{\partial(t_1)}{\partial x} + U_1.N_1.P.(T - t_1)}{\rho_t.cp_t.N_1.A_t} \quad (11)$$

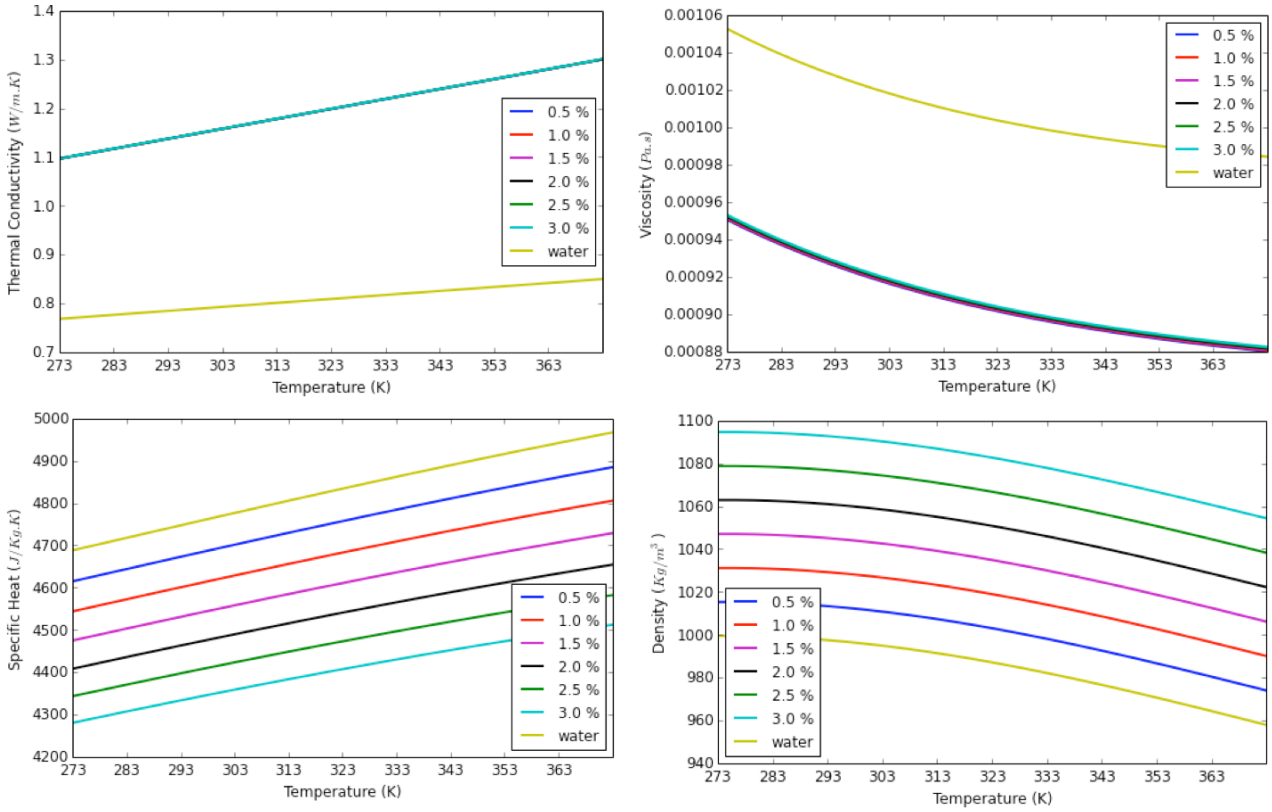

Figure 4: Physical properties for TiO_2 nanofluid.

- **Energy balance for the second tube-side pass**

$$\frac{\partial(t_2)}{\partial t} = \frac{-w.cp_t \frac{\partial(t_2)}{\partial x} + U_2.N_2.P.(T - t_2)}{\rho_t.cp_t.N_2.A_t} \quad (12)$$

- **Energy balance for the shell-side pass**

$$\frac{\partial(T)}{\partial t} = \frac{W.Cp\frac{\partial(T)}{\partial x} - U_1.N_1.P.(T - t_1) - U_2.N_2.P.(T - t_2)}{\rho_c.cp_c.A_c} \quad (13)$$

4. RESULTS AND DISCUSSION

The presented differential model was applied in a performance study of a TiO_2/water nanofluid used as a heat transfer fluid. Since a TiO_2/Water nanofluid may have varied concentrations of TiO_2 nanoparticles, the relevant physical properties were correlated as a function of temperature and TiO_2 concentration, as presented in Figure **4**.

The concentration change of TiO_2 was verified to have no influence on the thermal conductivity and viscosity, but they are significantly different when compared to pure water, which may result significant deviations if the presence of the nanoparticles is ignored, even for small concentrations. The specific heat and density showed a gradual variation with the concentration of TiO_2 nanoparticles.

Notice that the thermal conductivity and specific heat varies linearly with the temperature, allowing the use of a simple arithmetic mean of the heat exchanger terminal temperatures when applying an integrated design method (non-differential) such as Kern's or Bell−Delaware for heat exchanger dimensioning or analysis. Conversely, the viscosity and density have shown nonlinear behavior with temperature, therefore the application of an arithmetic mean of the process temperatures may not be acceptable for a large temperature variation due to the significant error that might be involved. In such case, the use of the mean caloric temperatures developed by Colburn *et al.* [2] is recommended.

In this work, two case-studies for the influence of the TiO_2 concentration on the thermo-fluid dynamics profiles of a 1-2 shell-and-tubes heat exchanger are developed. Process conditions for both case-studies are presented in Table **1**, while the heat exchanger specifications are shown in Table **2**. Table **3** summarizes the output data for the calculations of

Table 1: Process Operating Conditions

	Entrance Temperature (K)	Flow Rate (kg/s)	Fluid (Case-study 1)	Fluid (Case study 2)
Shell	340	40	water	water
Tubes	280	20	TiO_2/water, $\phi \leq 3\%$	water

water/nanofluid (Case 1) and water/water (Case 2), in a better way to point out their discrepancies.

Table 2: Heat Exchanger Specifications

Baffle spacing (m)	0.3
Tube pitch (m)	0.023
Tube count (TEMA)	160
Effective length (m)	5.0
Tube layout	triangular
Baffle cut	25%
Inner diameter – shell (m)	0.387
Inner diameter – tubes (m)	0.015
Outer diameter – shell (m)	0.4
Outer diameter – tubes (m)	0.019

From Table **3**, the correction factors for the logarithmic mean are within the recommended $F_t > 0.75$ range, and the true mean shows a small deviation compared to the logarithmic mean multiplied by its correction factor, indicating the consistency of temperature differences calculated.

Figure **5** presents steady state temperature profiles through the heat exchanger for both cases, in order to observe TiO_2 concentration influence. The results indicate a significant effect caused by the TiO_2 nanoparticles on the heat exchanger performance, even at small concentrations. With the nanofluid, the temperature approach at the heat exchanger outlet suffered a decrease of about 68%, varying from 19.02 °C (water) to 6.04 °C (water/TiO_2). The nanoparticles improved heat load in about 24%, which may yield an important reduction of equipment acquisition capital costs.

Table 3: Performance Output for Case Studies 1 and 2

Case 1: water/nanofluid	q (W): 3.24E+6 True Mean Temp. Diff. (K) = 28.28 Log. Mean Temp. Diff. (K) = 31.92 Arith. Mean Temp. Diff. (K) = 33.02 R: 0.45 P: 1.64 Ft: 0.89 T1 (out): 323.32 <--T1 (in): 340.00 T2 (in): 280.00 -->T2 (return): 305.08 T2 (out): 317.28 <--T2 (return): 305.08
Case 2: water/water	q (W): 2.61E+6 True Mean Temp. Diff. (K) = 37.47 Log. Mean Temp. Diff. (K) = 39.09 Arith. Mean Temp. Diff. (K) = 39.51 R: 0.49 P: 0.85 Ft: 0.96 T1 (out): 326.55 <-- T1 (in): 340.00 T2 (in): 280.00 --> T2 (return): 296.38 T2 (out): 307.53 <-- T2 (return): 296.38

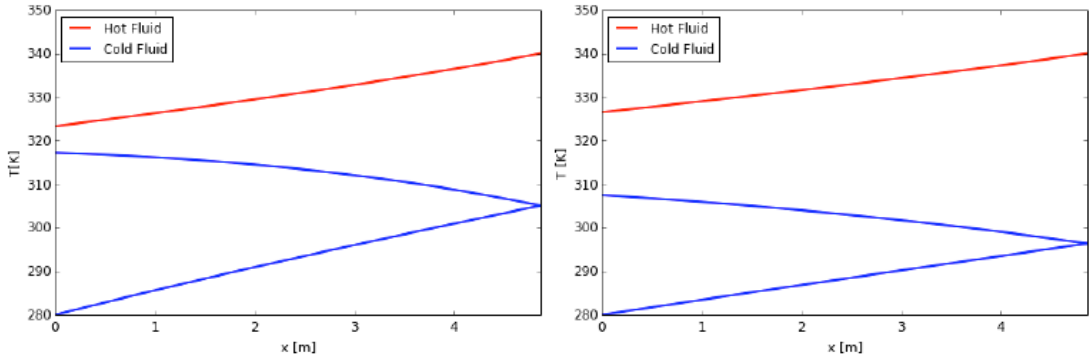

(**a**) (**b**)

Figure 5: Steady state temperature profiles: (**a**) Case 1 and (**b**) Case 2.

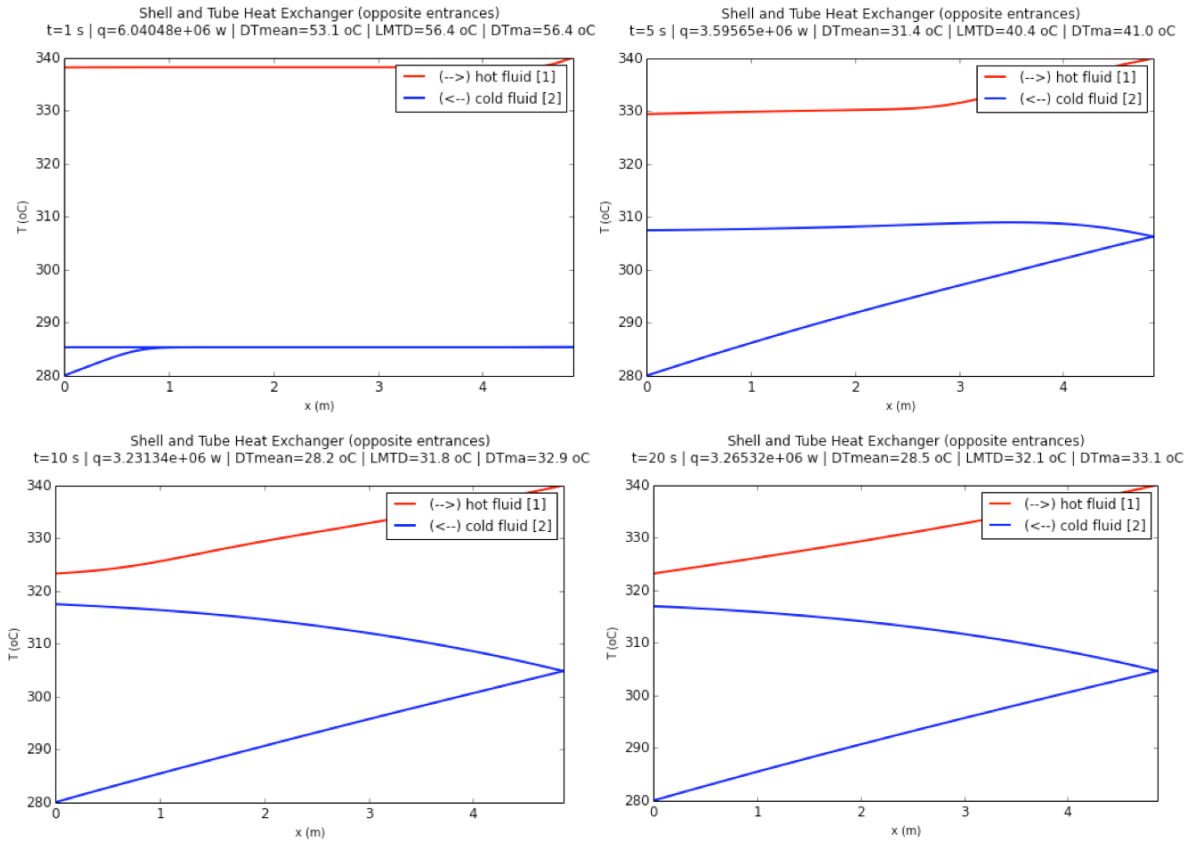

Figure 6: Transient temperature profiles through the heat exchanger: Case 1.

The model allows the study of the transient behavior of the heat exchanger, and the effect of the TiO_2 nanofluid on its startup is discussed with Figures **6** and **7**, which shows instantaneous temperature profiles along the exchanger for selected times. By comparison, we can see that the addition of TiO_2 to water does not alter the transient behavior in great extent, indicating that the response time to perturbations in the operating conditions are about the same with or without the nanofluid. This information has valuable practical importance once it supports that the adoption of the water/TiO_2 mixture in existing equipment should not bring additional complications to the legacy control systems already in place.

The transient response may be analyzed with the plots shown in Figure **8**(**a**) and (**b**), where only the exit fluid temperatures and the fluid temperature at the return head is plotted against time. For both case studies, the steady state takes approximately 15 seconds to settle; therefore the nanoparticles had no noticeable effect in this aspect. This result can be explained by the relatively high flow rates and low viscosity fluids employed in both cases analyzed.

Figures **9** and **10** bring the distributions of several physical properties along the heat exchanger length at steady state. The temperature profiles for thermal conductivity, density, viscosity and specific heat are almost linear for the entire exchanger, what indicates that a simple arithmetic mean of the fluids temperatures at the terminals could be used for evaluation of these properties without substantial errors.

As seen from Figure **4**, the TiO_2 nanoparticles lowers de viscosity and increases to some extent the thermal conductivity. This effect causes the inversion of the respective profiles in Figure **9,** where the lines for thermal conductivity and viscosity appears in opposite positions in comparison with Figure **10.** The phenomenon is similar for the larger density of the nanofluid mixture. Such changes in the physical properties, in contrast to plain water, are responsible for the improved performance of the heat exchanger, since for the same flow rate, the fluid dynamic pattern is shifted more into the turbulent regime, resulting in better heat transfer coefficients.

The overall heat transfer coefficients between the shell fluid and the first (U_1) and second (U_2) tube

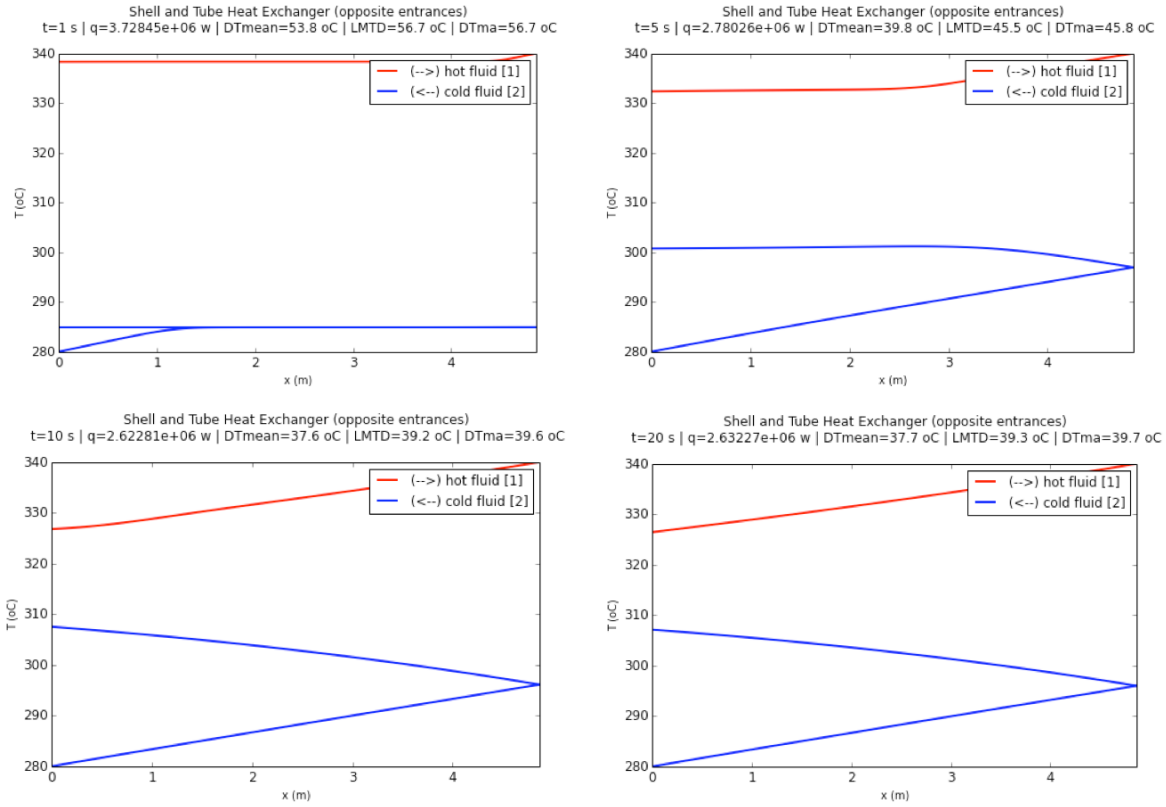

Figure 7: Transient temperature profiles through the heat exchanger: Case 2.

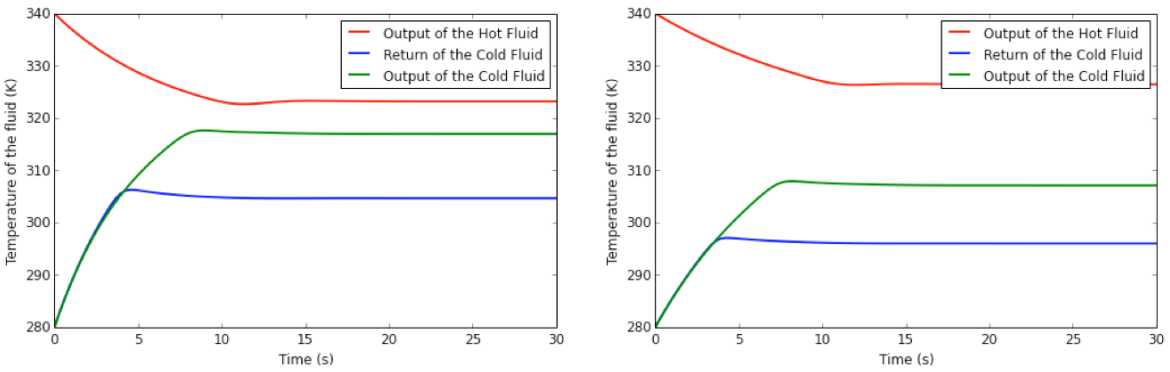

(**a**) (**b**)

Figure 8: Temperature variation with time at hot and cold fluid outlets and return head: (**a**) Case 1 e (**b**) Case 2.

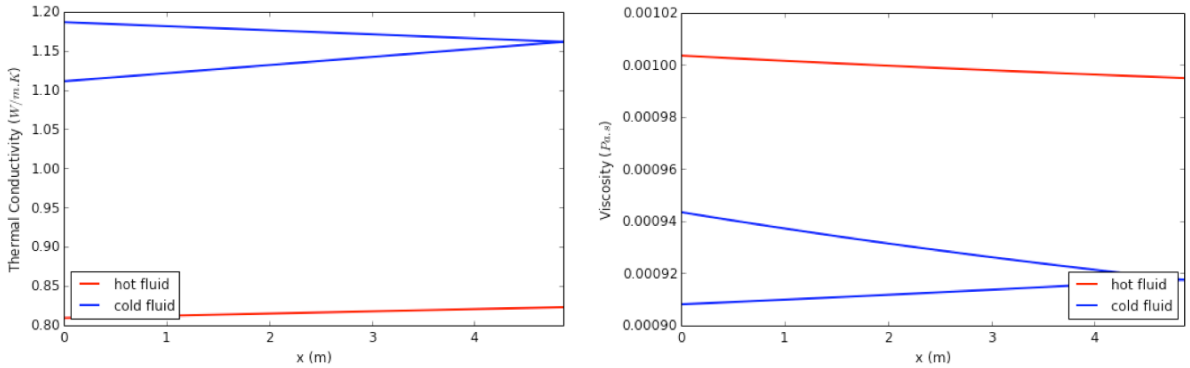

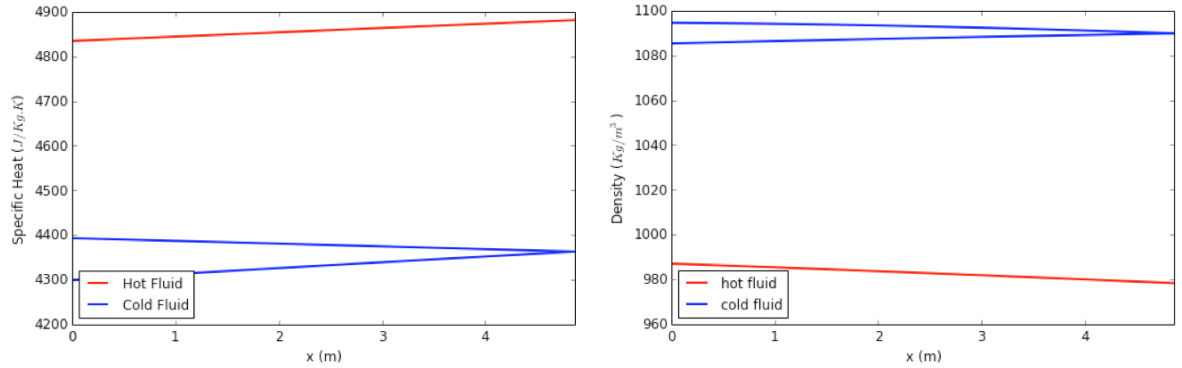

Figure 9: Variation of fluid physical properties along the heat exchanger: Case 1.

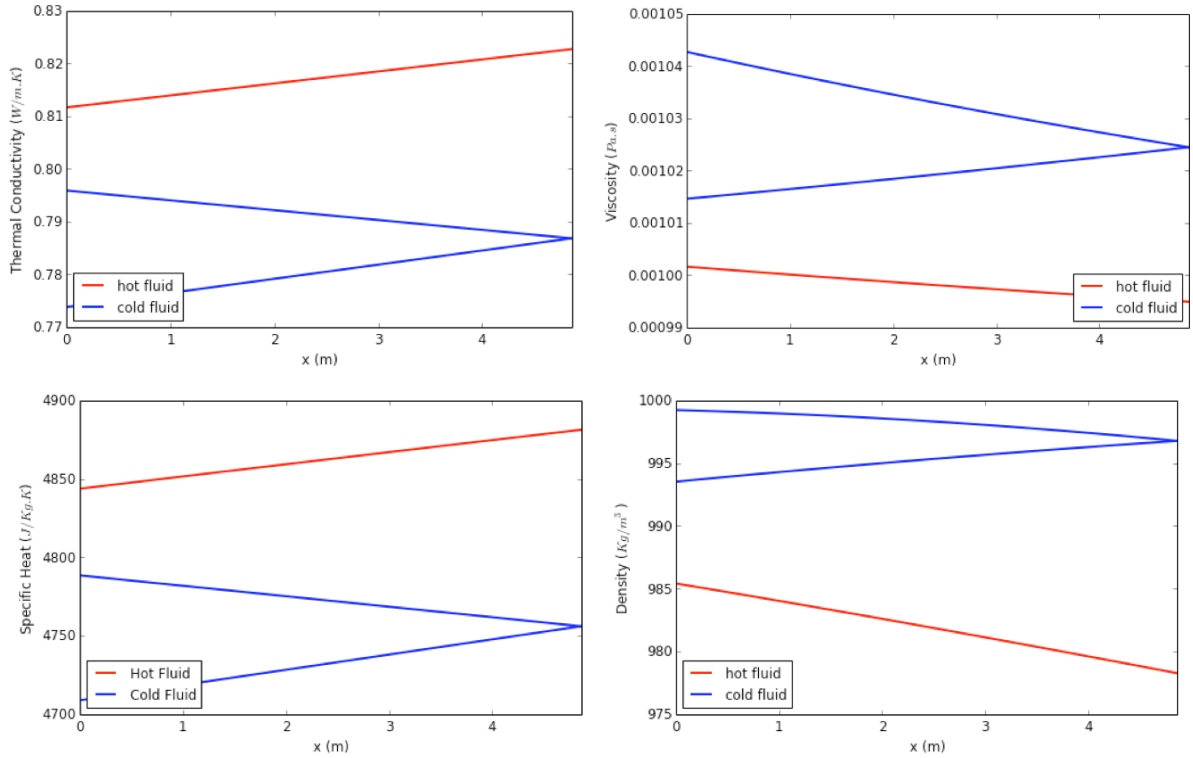

Figure 10: Variation of fluid physical properties along the heat exchanger: Case 2.

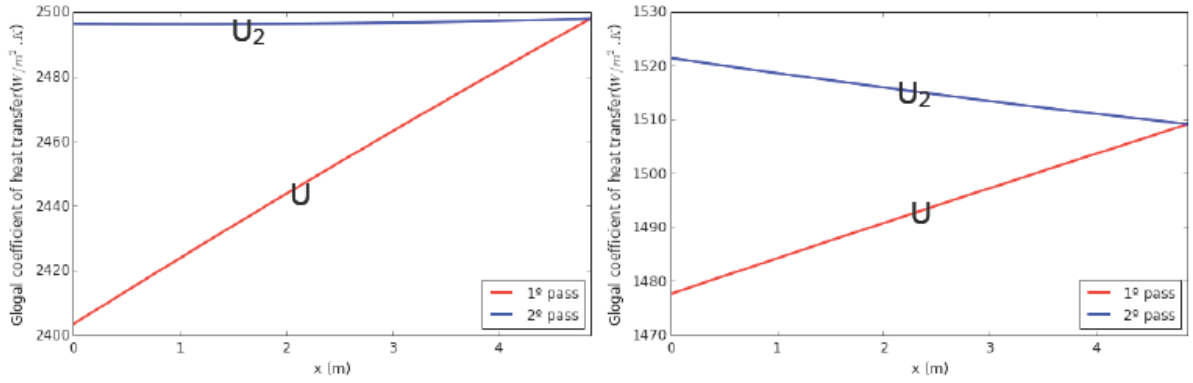

(**a**) (**b**)

Figure 11: Global coefficient profiles through the heat exchanger: (**a**) Case 1 e (**b**) Case 2.

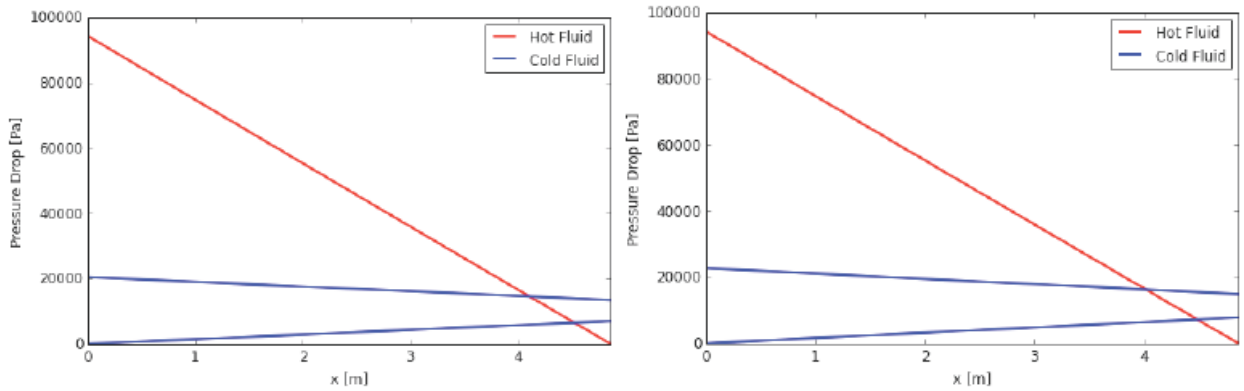

Figure 12: Typical pressure drop profile along the heat exchanger length.

passes are depicted by Figure **11.** The case study 1 (TiO_2/water) is caracterized by a faster increase of U_1 in the first pass and a posterior stabilization on the second one. As the two fluids have low viscosities and cold fluid flow rate (nanofluid or water) is half of hot fluid (water), the cold fluid controls heat transfer process.

To illustrate the ability of the model to estimate the differential pressure drop,

Figure **12**(**a**) and (**b**) brings the pressure drop profiles for both case studies discussed herein. Since the friction factor is a function of Reynolds number, which depends on the fluid density and viscosity, the local variation due to temperature changes can be captured.

5. CONCLUSION

This paper presents a time dependent one-dimensional differential version of the widely used Bell-Delaware method, which accepts local variation of physical properties and overall heat transfer coefficients. The developed model allows the analyses and design of 1-2 shell-and-tube heat exchangers with fractional baffles, being able to take into account any design parameter covered by the standard Bell-Delaware method.

For a practical application, the model was used to evaluate the performance of a TiO_2/water mixture utilized as a thermal nanofluid. The results indicate that disregarding the effect of TiO_2 nanoparticles even in small concentrations may lead to significant oversizing.

The linear variation of physical properties for low-viscosity fluids has been confirmed in both case studies, supporting the widely accepted practice of using fluid mean temperatures for sizing/analyzing tubular heat exchangers through the integrated method (non-differential). The arithmetic averages may not be appropriate to more viscous fluids, in which case the method of “caloric average” temperatures developed by Colburn *et al*. [2] is recommended.

The results show that the heat transfer performance can be improved significantly by the use of the water/TiO_2 nanofluid. The addition of nanoparticles in an amount as small as 3% increased the heat exchanger load in about 24%, which may translate directly to substantial reduction in acquisition and operating costs.

The simulations in this work were performed using the computational environment Python / IPython Notebook associated with some of their scientific modules, which has proven to be a valuable and versatile tool for computing studies.

NOMENCLATURE

A_c	shell cross area [m^2]
A_t	tube cross area [m^2]
C_p	hot fluid heat capacity [J/Kg.K]
c_p	cold fluid heat capacity [J/Kg.K]
d_p	particle diameter [m]
f	friction factor
h	film coefficient [W/m²K]
h_c	shell-side true film coefficient [W/m²K]
h_{ideal}	ideal tube bundle film coefficient [W/m²K]
J_c	window flow correction factor
J_L	leakage effect correction factor

J_b	bypass effect correction factor
J_R	external baffles distancing effects correction factor
J_S	laminar flow effect correction factor
J_μ	wall viscosity variation effect correction factor
k	thermal conductivity [w/m.k]
N_1	amount of heat exchanger first passage tubes
N_2	amount of heat exchanger second passage tubes
P	external tube perimeter (m)
ΔP_C	crossed flow pressure drop [Pa]
ΔP_w	window distancing pressure drop [Pa]
ΔP_e	input and output pressure drop [Pa]
ΔP_{total}	total shell-side pressure drop [Pa]
R_e	Reynolds number
t_1	first passage cold fluid local temperature [K]
t_2	second passage cold fluid local temperature [K]
T	hot fluid temperature [K]
U_1	first passage convection coefficient [W/m².K]
U_2	second passage convection coefficient [W/m².K]
w	cold fluid mass flow [Kg/s]
W	hot fluid mass flow [Kg/s]

Greek Letters

μ	fluid viscosity at the flow temperature [Pa.s]
ρ	fluid density [Kg/m³]

Subscript

t	tube
c	shell
nf	nanofluid
f	fluid

REFERENCES

[1] TABOREK. Shell-and-Tube Heat Exchangers. Section 3.3, Heat Exchanger Design Handbook. Hemisphere (1983).

[2] COLBURN AP, DE E, du P. Mean temperature difference and heat transfer coefficient in liquid heat exchangers. Industrial and Engineering Chemistry 1993; 25(8): 873-877. ACS Publications.

[3] SIEDER EN, TATE CE. Heat Transfer and Pressure Drop of Liquids in Tubes. Industrial and Engineering Chemistry 1936; 28: 1429-1433. http://dx.doi.org/10.1021/ie50324a027

[4] TINKER T. Shell side characteristics of shell and tube heat exchangers: a simplified rating system for commercial heat exchanger. J Heat Transfer 195880; p. 36-52: 1958.

[5] BELL KJ. Final Report of the Cooperative Research Program on shell-and-tube heat exchangers. University of Delaware Eng Exp Sta Bulletin 1963; 5.

[6] RIBEIRO CMC. Comparação de Métodos e Cálculo Termo-Hidraúlico para Trocados de Calor Casco e Tubo sem Mudança de Fase. Tese de Mestrado-FEC/UNICAMP 1984.

[7] BELL KJ. Delaware Method for Shell Side Design. Heat Exchanger Thermal-Hydraulic Fundamentals and Design. New York: McGraw-Hill 1980.

[8] KERN DQ. Process Heat Transfer. New York: McGraw-Hill 1950.

[9] Xuan Y, Roetzel W. Conceptions for heat transfer correlation of nanofluids. Int J Heat Mass Trans. 43 2000; 3701-3707. http://dx.doi.org/10.1016/S0017-9310(99)00369-5

[10] Sharma KV, Sarma PK, Azmi WH, Mamat R, Kadirgama K. Correlations to predict friction and forced convection heat transfer coefficients of water based nanofluids for turbulent flow in a tube. Int J Microscale Nanoscale Therm. Fluid Transport Phenom. (Special Issue in Heat and Mass Transfer in Nanofluids) 2012; 3 (4): 1-25.

[11] Azmi WH, Sharma KV, Sarma PK, Mamat R, Anuar S, Dharma Rao V. Experimental determination of turbulent forced convection heat transfer and friction factor with SiO2 nanofluid. Exp Therm Fluid Sci 2013; 51 (0): 103e 111.

Received on 13-11-2014 Accepted on 22-11-2014 Published on 15-01-2015

DOI: http://dx.doi.org/10.15377/2409-5826.2015.02.01.2